

1

2           The transcription factor IscR promotes *Yersinia* type III secretion system activity by  
3                           antagonizing the repressive H-NS-YmoA histone-like protein complex

4

5 David Balderas<sup>1</sup>, Pablo Alvarez<sup>1</sup>†, Mané Ohanyan<sup>1</sup>, Erin Mettert<sup>2</sup>, Natasha Tanner<sup>1</sup>, Patricia J. Kiley<sup>2</sup>, and  
6 Victoria Auerbuch<sup>1\*</sup>

7

8 <sup>1</sup>Department of Microbiology and Environmental Toxicology, University of California, Santa Cruz, Santa Cruz,  
9 California, USA

10

11 <sup>2</sup> Department of Biomolecular Chemistry, University of Wisconsin-Madison, Madison, Wisconsin, USA

12 †Present Address: Pablo Alvarez, Department of Microbiology, Immunology & Molecular Genetics, University  
13 of California, Los Angeles, Los Angeles, California, USA

14

15 **Author Contributions:**

16 DB, VA, and PK designed the study. DB, PA, EM, NT, and MO performed the experiments. DB, PA, EM, NT,  
17 and MO performed data analysis. DB, PA, VA, and PK wrote the paper.

18

19 **Competing Interest Statement:**

20 *The authors declare that the research was conducted in the absence of any commercial or financial*  
21 *relationships that could be construed as a potential conflict of interest.*

22

23 \* **Correspondence:** Victoria Auerbuch; [vastone@ucsc.edu](mailto:vastone@ucsc.edu)

24 **Section:** Prokaryotic genetics

25 **Keywords:** *Yersinia*, *Yersinia pseudotuberculosis*, type III secretion system, IscR, H-NS, YmoA

## 26 **Abstract**

27 The type III secretion system (T3SS) is a appendage used by many bacterial pathogens, such as pathogenic  
28 *Yersinia*, to subvert host defenses. However, because the T3SS is energetically costly and immunogenic, it  
29 must be tightly regulated in response to environmental cues to enable survival in the host. Here we show that  
30 expression of the *Yersinia* Ysc T3SS master regulator, LcrF, is orchestrated by the opposing activities of the  
31 repressive YmoA/H-NS histone-like protein complex and induction by the iron and oxygen-regulated IscR  
32 transcription factor. Although IscR has been shown to bind the *lcrF* promoter and is required for *in vivo*  
33 expression of *lcrF*, in this study we show IscR alone fails to enhance *lcrF* transcription *in vitro*. Rather, we find  
34 that in a *ymoA* mutant, IscR is no longer required for LcrF expression or T3SS activity. Additionally, a mutation  
35 in YmoA that prevents H-NS binding (*ymoA*<sup>D43N</sup>) rescues the T3SS defect of a  $\Delta$ *iscR* mutant, suggesting that a  
36 YmoA/H-NS complex is needed for this repressive activity. Furthermore, chromatin immunoprecipitation  
37 analysis revealed that H-NS is enriched at the *lcrF* promoter at environmental temperatures, while IscR is  
38 enriched at this promoter at mammalian body temperature under aerobic conditions. Importantly, CRISPRi  
39 knockdown of H-NS leads to increased *lcrF* transcription. Collectively, our data suggest that as IscR levels rise  
40 with iron limitation and oxidative stress, conditions *Yersinia* experiences during extraintestinal infection, IscR  
41 antagonizes YmoA/H-NS-mediated repression of *lcrF* transcription to drive T3SS activity and manipulate host  
42 defense mechanisms.

43

## 44 **Author Summary**

45 Facultative pathogens must silence virulence gene expression during growth in the environment, while  
46 retaining the ability to upregulate these genes upon infection of a host. H-NS is an architectural DNA binding  
47 protein proposed to silence horizontally acquired genes, regulating virulence genes in a number of pathogens.  
48 Indeed, H-NS was predicted to regulate plasmid-encoded virulence genes in pathogenic *Yersinia*. However,  
49 *Yersinia* H-NS is reported to be essential, complicating testing of this model. We used chromatin  
50 immunoprecipitation and inducible CRISPRi knockdown to show that H-NS binds to the promoter of a critical  
51 plasmid-encoded virulence gene, silencing its expression. Importantly, under conditions that mimic *Yersinia*  
52 infection of a mammalian host, the transcriptional regulator IscR displaces H-NS to drive virulence factor  
53 expression.

54

55

## 56 Introduction

57 Virulence factors are critical components that allow pathogens to establish or sustain infections within a given  
58 host. One common bacterial virulence factor is a needle-like apparatus, known as the type III secretion system  
59 (T3SS) (1,2). Enteropathogenic *Yersinia pseudotuberculosis* is one of three human pathogenic *Yersinia* spp.  
60 that use the T3SS to inject effector proteins into host cells that dampen host immune responses, facilitating  
61 extracellular growth (3–6). Members of human pathogenic *Yersinia* spp. include *Yersinia pestis*, the causative  
62 agent of plague, and the enteropathogens *Yersinia enterocolitica* and *Yersinia pseudotuberculosis*. While the  
63 T3SS is critical for infection, this apparatus appears to be metabolically burdensome since constitutive  
64 expression of the T3SS leads to growth arrest (7,8). In addition, the Ysc T3SS is associated with pathogen-  
65 associated molecular patterns (PAMPs) recognized by several innate immune receptors, and some of these  
66 T3SS-associated PAMPs have evolved under selective evolutionary pressure by the ensuing immune response  
67 (5,9). Without tight regulation of T3SS expression and deployment, these metabolic and immunological burdens  
68 would decrease the chance of *Yersinia* survival in the host.

69

70 The Ysc T3SS is encoded on a 70 kb plasmid for *Yersinia* Virulence, known as pYV or pCD1 (10). Transcriptional  
71 regulation of T3SS genes is maintained by a master regulator called LcrF/VirF (11–14). LcrF itself is also  
72 encoded on pYV, within the *yscW-lcrF* operon, and is highly conserved among all three human pathogenic  
73 *Yersinia* spp. LcrF is part of a larger family of AraC-like transcriptional regulators, and orthologs exist in other  
74 T3SS-encoding pathogens, such as ExsA in the nosocomial pathogen *Pseudomonas aeruginosa* (15). The  
75 *yscW-lcrF* operon is regulated at various stages in response to different environmental stimuli, including  
76 temperature, oxygen, and iron availability (16,17). For example, an RNA thermometer blocks the ribosome  
77 binding site of *lcrF* at room temperature, but melts at mammalian body temperature, allowing *lcrF* translation  
78 (16).

79

80 In addition, transcriptional control of *yscW-lcrF* has been predicted to be mediated by the Histone-like Nucleoid  
81 structuring protein, H-NS (16). H-NS contains an N-terminal oligomerization domain and a C-terminal DNA  
82 minor-groove binding domain separated by a flexible linker (18,19). H-NS preferentially binds AT rich regions of

83 DNA (19,20). Once H-NS binds a high-affinity site, H-NS oligomerizes on the DNA (21,22). H-NS oligomers can  
84 either form a nucleoprotein filament on a contiguous stretch of DNA, or H-NS can form DNA bridges when  
85 multiple discrete H-NS binding regions are brought together, either way leading to transcriptional silencing of  
86 that particular gene (23). Interestingly, H-NS in multiple bacterial pathogens has been shown to silence certain  
87 gene targets during growth outside of the mammalian host (20-30°C), but fails to silence these same targets to  
88 the same magnitude when exposed to mammalian body temperature (37°C) (24–26). This suggests H-NS may  
89 play a role in repressing virulence factors outside host organisms in facultative pathogens. However, H-NS has  
90 been suggested to be an essential gene in pathogenic *Yersinia* (27,28), making it challenging to definitively test  
91 the role of H-NS in regulating gene expression in these organisms. Additionally, YmoA (“*Yersinia modulator*”) in  
92 *Y. pseudotuberculosis*, an *E. coli* Hha (“high hemolysin activity”) ortholog, has been suggested to modulate H-  
93 NS repression of a subset of promoters and deletion of *ymoA* in *Yersinia* leads to changes in gene expression  
94 of putative H-NS targets (16,29–31). YmoA and Hha lack a DNA binding domain; instead, these proteins form  
95 a heterocomplex with H-NS or H-NS paralogs (32–35). Recent data has suggested that Hha contributes to H-  
96 NS silencing by aiding in H-NS bridging (36). In the plague agent *Yersinia pestis*, YmoA is suggested to have a  
97 higher turnover rate at 37°C compared to environmental temperatures (30). While YmoA alone cannot bind the  
98 *yscW-lcrF* promoter, H-NS alone or the YmoA/H-NS complex can (16). Current models suggest that degradation  
99 of YmoA and therefore a reduction in the YmoA/H-NS complex at 37°C relieves repression of *yscW-lcrF* (30).  
100 Yet, *ymoA* deletion mutants exhibit even higher levels of T3SS expression at 37°C compared to a parental strain  
101 in all three pathogenic *Yersinia* species (16,29,30), suggesting that some YmoA is present even at 37°C during  
102 mammalian infection.

103  
104 The Iron Sulfur Cluster Regulator IscR is a critical positive regulator of *lcrF* (17,37). IscR belongs to the Rrf2  
105 family of winged helix-turn-helix transcription factors (38,39). IscR was first characterized in *E. coli* where it  
106 exists in two forms: holo-IscR bound to a [2Fe-2S] cluster, and cluster-less apo-IscR (40–43). Both forms of  
107 IscR bind DNA, but while both apo-IscR and holo-IscR bind to so-called type II motif sequences, only holo-IscR  
108 binds type I motifs (41,42) Holo-IscR represses its own expression through binding two type I motifs in the *isc*  
109 promoter (44). Thus, conditions that increase iron-sulfur cluster demand, such as iron starvation or oxidative  
110 stress, lead to a lower holo- to apo-IscR ratio and higher overall IscR levels. *E. coli* IscR has been shown to  
111 activate or repress transcription of target genes *in vitro* and *in vivo* (41). We have previously shown that low iron

112 and oxidative stress lead to upregulation of *IscR* in *Yersinia*, and subsequently upregulation of *IcrF* transcription  
113 and T3SS expression (17,37). Although we have shown *IscR* must bind upstream of the *yscW-IcrF* promoter to  
114 promote *IcrF* expression, the mechanism by which *IscR* promotes *IcrF* transcription is unknown. In this study,  
115 we find that *IscR* does not enhance *in vitro* transcription of *yscW-IcrF* mRNA. Instead, we show that *IscR*  
116 antagonizes YmoA/H-NS repression of the *yscW-IcrF* promoter to induce type III secretion.

117

## 118 **Results**

### 119 ***IscR* does not promote *IcrF* transcription *in vitro***

120 *IscR* has previously been shown to enhance transcription by directly activating RNA polymerase activity or by  
121 antagonizing transcriptional repressors (41,45). To determine the molecular mechanism by which *IscR*  
122 potentiates transcription of *yscW-IcrF*, we performed an *in vitro* transcription assay with a DNA fragment  
123 containing the wild-type *Y. pseudotuberculosis yscW-IcrF* promoter (-143 to +58 bp relative to the +1  
124 transcription start site) and the *IscR* binding site. Surprisingly, no change in *yscW-IcrF* transcription was  
125 observed after addition of apo-*IscR* (Fig 1). However, *IscR* was able to promote transcription of both *Y.*  
126 *pseudotuberculosis sufA* and *E. coli sufA*. These data suggest that *IscR* does not enhance *yscW-IcrF*  
127 transcription by regulating RNA polymerase directly. We therefore hypothesized that *IscR* promotes *yscW-IcrF*  
128 expression by antagonizing a repressor.

129

### 130 ***IscR* is not required for *LcrF* expression or type III secretion in 131 the absence of YmoA**

132 Loss of *iscR* leads to a profound defect in T3SS activity while disruption of *ymoA* causes enhanced T3SS  
133 activity (16,17,37,46,47). We therefore hypothesized that *IscR* antagonizes YmoA-dependent repression of the  
134 T3SS. To test this, we assessed T3SS activity of *Y. pseudotuberculosis* expressing or lacking *iscR* and/or  
135 *ymoA*. Consistent with previous studies, we observed ~18-fold decrease in secretion of the T3SS effector  
136 protein YopE upon *iscR* deletion, while *ymoA* deletion led to ~6-fold increase in YopE secretion (Fig 2A). As  
137 expected for this transcriptional circuit, the effect of YmoA on T3SS activity required *LcrF*, the direct regulator

138 of the T3SS (Fig S1). Importantly, YopE secretion in the  $\Delta iscR/\Delta ymoA$  double mutant was similar to  $\Delta ymoA$   
139 mutant, indicating that IscR is dispensable for T3SS activity in the absence of YmoA (Fig 2A).  
140 Proteins of the YmoA family lack a DNA binding domain and are thought to affect transcription by its interaction  
141 with the histone like protein H-NS (31,36). Previous work has shown that a complex of YmoA/H-NS, but not  
142 YmoA alone, binds the *yscW-lcrF* promoter (16). To test the requirement for a YmoA/H-NS complex in regulation  
143 of YopE secretion by IscR we made use of a YmoA D43N mutant, which cannot interact with H-NS *in vitro* (48)  
144 and which we showed was produced in *Y. pseudotuberculosis* (Fig S2). Indeed, a *ymoA*<sup>D43N</sup> mutant exhibited  
145 ~6-fold increase in YopE secretion similar to a *ymoA* deletion (Fig 2A). This suggests that YmoA represses  
146 *yscW-lcrF* through its interaction with H-NS. Furthermore, there was no difference in YopE secretion between  
147 the *ymoA*<sup>D43N</sup> mutant and the *iscR/ymoA*<sup>D43N</sup> double mutant. These effects on YopE secretion are most easily  
148 explained by changes in *lcrF* transcription and accordingly, LcrF protein levels. Indeed, while the  $\Delta iscR$  mutant  
149 had a ~5-fold reduction in *lcrF* mRNA compared to wildtype and the  $\Delta ymoA$  and *ymoA*<sup>D43N</sup> mutants displayed  
150 ~10-fold elevated *lcrF* mRNA, we observed no difference in *lcrF* mRNA levels between the  $\Delta ymoA$  and  
151  $\Delta iscR/\Delta ymoA$  mutants (Fig 2B). Accordingly, we observed no difference in LcrF protein levels when *iscR* was  
152 deleted from the *ymoA* mutants (Fig 2C). Collectively, these data suggest that YmoA requires H-NS binding to  
153 inhibit *lcrF* transcription, and that IscR only exerts its positive effect on *lcrF* transcription in the presence of the  
154 YmoA/H-NS complex.

155

156

## 157 **IscR binding to the *yscW-lcrF* promoter is critical for LcrF** 158 **expression only in the presence of YmoA**

159 As IscR did not modulate YmoA or H-NS expression (Fig S3), we hypothesized that IscR must directly regulate  
160 LcrF by binding to the *yscW-lcrF* promoter to antagonize YmoA/H-NS-mediated repression. In order to test  
161 whether IscR binding to the *yscW-lcrF* promoter is important for regulating LcrF expression in the presence of  
162 YmoA, we used a previously characterized IscR binding site mutant (*lcrF*<sup>PNull</sup>) that ablates IscR binding to the  
163 *yscW-lcrF* promoter but expresses wildtype IscR (17). As expected, the *lcrF*<sup>PNull</sup> exhibited a ~5-fold reduction in  
164 *lcrF* mRNA similar to what was observed in an *iscR* deletion mutant (Fig 3A). LcrF protein was completely  
165 undetectable in the *lcrF*<sup>PNull</sup> compared to the wildtype strain (Fig 3B). However, in the absence of *ymoA*, this

166 reduction in LcrF expression or T3SS activity by the *IcrF*<sup>ΔNull</sup> mutation was eliminated (Fig 3A-C). Taken together,  
167 these data suggest that IscR-dependent activation of LcrF expression in the presence of YmoA requires direct  
168 binding of IscR to the *yscW-IcrF* promoter.

169

## 170 **Knockdown of H-NS leads to derepression of LcrF**

171 We next examined the role of H-NS in the regulation of *IcrF* expression. H-NS has been proposed to be  
172 essential in both *Y. pseudotuberculosis* and *Y. enterocolitica* (27,28). Therefore, in order to test whether  
173 reducing H-NS occupancy at the *yscW-IcrF* promoter affects LcrF expression, we used CRISPRi to  
174 knockdown H-NS expression in wildtype *Y. pseudotuberculosis* and measured *IcrF* expression levels. For this  
175 CRISPRi system pioneered in *Yersinia pestis* (49), target gene guide RNAs and dCas9 can be induced in the  
176 presence of anhydrotetracycline (aTC). CRISPRi knockdown led to a ~6-fold decrease in H-NS transcription  
177 when exposed to aTC (Fig 4A). Importantly, this reduction of H-NS expression led to a ~31-fold increase in  
178 *IcrF* mRNA, suggesting H-NS represses LcrF transcription (Fig 4B). Knockdown of H-NS did not affect  
179 expression of *gyrA*, a housekeeping gene which is not predicted to be regulated by H-NS (Fig 4C). These data  
180 provide the first direct evidence that H-NS negatively influences *Yersinia* LcrF expression.

181

## 182 **Two H-NS binding sites are required to repress *yscW-IcrF*** 183 **promoter activity**

184 H-NS and YmoA/H-NS complexes have been shown *in vitro* to bind the *yscW-IcrF* promoter between the -2 to  
185 the +272 position relative to the transcriptional start site (16). However, the exact H-NS binding site was not  
186 identified. We used FIMO-MEME suite tools to predict putative H-NS binding sites upstream of *yscW-IcrF* and  
187 identified three predicted H-NS binding sites (p-value < 10<sup>-3</sup>; Fig 5A). These data suggested that H-NS may form  
188 a DNA bridge at this locus and repress *yscW-IcrF* transcription (50,51). To characterize which regions of the  
189 *yscW-IcrF* promoter allow for H-NS-YmoA repression and IscR activation, we systematically truncated the *yscW-*  
190 *IcrF* promoter and tested promoter activity using a *lacZ* reporter in the wildtype,  $\Delta$ *iscR*,  $\Delta$ *ymoA*, and  $\Delta$ *iscR*/ $\Delta$ *ymoA*  
191 backgrounds (Fig 5A). As expected, deletion of *ymoA* led to an increase in activity of the longest promoter  
192 construct, while *iscR* deletion led to a decrease in this promoter activity compared to the wildtype strain (Fig 5B).  
193 Consistent with our previous data showing that IscR was dispensable in the absence of YmoA, deletion of *iscR*

194 in a  $\Delta ymoA$  background did not inhibit the derepressed promoter activity seen in the  $\Delta ymoA$  background.  
195 Eliminating the most upstream predicted H-NS binding site did not affect promoter activity (promoter 1 compared  
196 to promoter 2). However, additional truncation of the second H-NS binding site led to an increase in promoter  
197 activity in the wildtype and  $\Delta iscR$  backgrounds, but not in the backgrounds lacking *ymoA* (promoter 2 compared  
198 to promoter 3) suggesting that some of the repressive effect by H-NS/YmoA had been lost. Importantly, further  
199 truncation to eliminate the IscR binding site led to deregulated promoter activity that was independent of IscR  
200 and YmoA (promoter 4). These data suggest that IscR is required to disrupt YmoA/H-NS repressive activity,  
201 explaining why it is dispensable in the absence of YmoA/H-NS. Lastly, truncation to eliminate the -35 and -10  
202 promoter elements led to a complete lack of promoter activity (promoter 5). Taken together, these data suggest  
203 that IscR binding to the *ycsW-lcrF* promoter antagonizes YmoA/H-NS repression.

204

205 To test whether H-NS binds to these predicted sites, we carried out ChIP-qPCR analysis to assess H-NS  
206 occupancy at the I, II, and III putative binding regions *in vivo*. In order to immunoprecipitate H-NS-DNA  
207 complexes, we used a chromosomally-encoded 3xFLAG tagged H-NS allele. This FLAG tag did not affect the  
208 ability of H-NS to repress *LcrF* expression (Fig S4). Interestingly, previous reports have shown that H-NS in  
209 other facultative pathogens represses the expression of certain virulence genes under environmental  
210 temperatures (<30°C) but exhibits decreased binding at mammalian body temperature (37°C) (24,26,52).  
211 Consistent with this, we could not detect H-NS binding at any of these predicted sites at 37°C, but did observe  
212 H-NS enrichment at all three predicted sites in the *ycsW-lcrF* promoter when bacteria were cultured at 26°C (Fig  
213 6A). In contrast, no enrichment of H-NS was seen at a control pYV-encoded promoter that was not predicted to  
214 bind H-NS at either temperature (DN756\_21750).

215

216 YmoA is predicted to affect the repressive ability of H-NS but was not shown to affect H-NS binding to the *ycsW-*  
217 *lcrF* promoter (16). Consistent with this, no difference in H-NS binding was observed in the *ymoA* mutant  
218 compared to the parental strain at 26°C, suggesting that YmoA does not affect H-NS occupancy at the *ycsW-*  
219 *lcrF* promoter at this temperature (Fig 6B). Likewise, there was no difference in H-NS enrichment at the *ycsW-*  
220 *lcrF* promoter between the *iscR* mutant and the wildtype strain at 26°C (Fig 6B) or 37°C (Fig 6C). It is possible  
221 that H-NS binds to the *ycsW-lcrF* promoter at 37°C, but this is below the limit of detection for ChIP-qPCR. Taken



222 together, these data suggest that H-NS occupies the *yscW-lcrF* promoter at high levels under environmental  
223 temperatures at which the T3SS is repressed.

224

225 We also measured IscR enrichment at the *yscW-lcrF* promoter *in vivo*. We used a chromosomal 3xFLAG tagged  
226 IscR allele previously shown not to affect IscR activity (53). Interestingly, IscR enrichment at the *yscW-lcrF*  
227 promoter was ~3-fold higher at 37°C compared to 26°C (Fig 6D). This increase in IscR binding is not due to  
228 increased IscR levels since we do not observe higher levels of IscR protein when cultured at 37°C compared to  
229 26°C (Fig S3), nor do we see increased binding of IscR at the promoter of another known IscR target, the *suf*  
230 operon (Fig S5). In addition, deletion of *ymoA* did not affect IscR occupancy at the *yscW-lcrF* promoter at 26°C  
231 or 37°C. These data suggest that at environmental temperatures, H-NS binds to the *yscW-lcrF* promoter at high  
232 levels and represses transcription, while at mammalian body temperature IscR binding to the *yscW-lcrF*  
233 promoter antagonizes residual YmoA/H-NS-mediated repression.

234

## 235 **Environmental cues that increase IscR levels enable** 236 **derepression of the *yscW-lcrF* promoter**

237 We previously showed that low iron and high oxidative stress lead to elevated IscR levels, which then activate  
238 the T3SS through upregulation of LcrF (17). The data shown here suggest that this increase in IscR levels may  
239 be necessary to antagonize repressive YmoA-H-NS-activity at the *yscW-lcrF* promoter. To test this model, we  
240 measured *lcrF* mRNA levels in  $\Delta$ *iscR* and  $\Delta$ *ymoA* mutants under aerobic or anaerobic conditions at 37°C. As  
241 expected, under aerobic conditions *iscR* mRNA levels were increased ~4-fold compared to anaerobic conditions  
242 (Fig 7A). This upregulation of *iscR* levels led to a ~12-fold induction in *lcrF* levels in the wildtype strain (Fig 7B).  
243 In contrast, *lcrF* mRNA and protein levels were not affected by oxygen in the  $\Delta$ *ymoA* and  $\Delta$ *iscR*/ $\Delta$ *ymoA* mutants  
244 (Fig 7A, 7C). It is important to note that deletion of *ymoA* reduced expression of IscR mRNA and protein  
245 expression under these conditions, although this does not explain elevated LcrF/T3SS expression in the *ymoA*  
246 mutant. Indeed, IscR occupancy at the *lcrF* promoter is not affected by *ymoA* deletion (Fig 6D). Taken together,  
247 these data suggest that environmental conditions that increase IscR levels (such as aerobic conditions) disrupt  
248 YmoA/H-NS-mediated repression of *lcrF* expression.

249

## 250 Discussion

251 Our data suggests IscR activates transcription of *yscW-lcrF* by antagonizing repressive activity of YmoA-H-NS  
252 (Fig 8). Knockdown of *hns* expression by CRISPRi revealed that H-NS, a putative essential gene in *Yersinia*, is  
253 required for repression of *yscW-lcrF*. Furthermore, YmoA must interact with H-NS to repress *yscW-lcrF*  
254 transcription and overall T3SS activity at 37°C. Importantly, IscR promotes *yscW-lcrF* expression and T3SS  
255 activity only in the presence of YmoA-H-NS repression. Our data point to a model where H-NS occupies the  
256 *yscW-lcrF* promoter at environmental temperatures independently of YmoA and IscR, but at mammalian body  
257 temperature YmoA binding to H-NS represses the *yscW-lcrF* promoter only when IscR levels are low (Fig 8). *Y.*  
258 *pseudotuberculosis* IscR levels are thought to be kept low in the intestinal lumen, under anaerobic iron-replete  
259 conditions. Under these conditions, where the T3SS is not required for colonization, YmoA and H-NS cooperate  
260 to repress LcrF expression. Once *Yersinia* cross the intestinal barrier, oxygen tension increases and iron is  
261 scarce, allowing elevated IscR levels that antagonize YmoA/H-NS activity to allow LcrF expression and type III  
262 secretion, which is required for extraintestinal infection (54–57). This suggests that YmoA/H-NS and IscR work  
263 together to allow temperature and oxygen tension/iron availability to limit T3SS activity not just to only inside the  
264 host organism, but to only in extraintestinal tissue. Given that IscR is essential for T3SS activity in the related  
265 plague agent *Y. pestis* that does not enter the intestinal tract (17), we predict that in the flea vector that maintains  
266 temperatures lower than the mammalian host, H-NS represses LcrF expression. Then upon entry into the  
267 mammalian host bloodstream, the elevated temperature leads to decreased occupancy of YmoA/H-NS at the  
268 *yscW-lcrF* promoter to levels that allow IscR to antagonize YmoA/H-NS repression and facilitate expression of  
269 the T3SS activity required for early stages of plague (58,59).

270  
271 Previous reports have suggested that H-NS targets a subset of genes under environmental conditions, but no  
272 longer represses those same genes under mammalian body temperature. For example, the *Shigella flexneri*  
273 T3SS is regulated by an AraC transcriptional regulator called VirF and H-NS (60,61). VirF promotes VirB, which  
274 ultimately activates the *Shigella* T3SS (62). The *Shigella* T3SS is only expressed under mammalian body  
275 temperature and this is controlled by preventing expression of VirF at environmental temperatures. Interestingly,  
276 H-NS was shown to directly repress *virF* transcription by binding to the *virF* promoter (52). Later studies found  
277 that H-NS binds to two distinct sites upstream of *virF* leading to the formation of a DNA bridge (63). This study  
278 also found that H-NS binds to a higher degree at the *virF* promoter under lower temperatures (<30°C) compared

279 to mammalian body temperature (37°C). Thus H-NS was shown to repress promoter activity of *virF* at both lower  
280 temperatures (<30°C) and mammalian body temperature (37°C), however H-NS has a stronger effect on  
281 repression of *virF* under lower temperatures (52). This molecular mechanism is similar to what we report here,  
282 where H-NS occupies the *yscW-lcrF* promoter at environmental conditions and is below the limit of detection by  
283 ChIP-qPCR at 37°C. However, *Yersinia* H-NS repression of LcrF still occurs at 37°C unless IscR levels increase  
284 sufficiently to antagonize this repression.

285  
286 YmoA was previously shown to bind to H-NS and the YmoA/H-NS complex was proposed to regulate LcrF  
287 expression (16,48). Indeed, a YmoA mutation that eliminates H-NS binding phenocopied the *ymoA* deficient  
288 strain, suggesting YmoA must interact with H-NS to repress LcrF/T3SS. However, YmoA was not shown to  
289 affect H-NS binding to the *yscW-lcrF* promoter *in vitro* (16), and our ChIP-qPCR analysis did not find a change  
290 in H-NS *yscW-lcrF* promoter occupancy in the presence or absence of YmoA at 26°C. At 37°C, H-NS occupancy  
291 was below the limit of detection by ChIP-qPCR, so we could not rule out H-NS or YmoA/H-NS binding to the  
292 *yscW-lcrF* promoter at this temperature. However, deletion of *ymoA* or knockdown of *hns* both caused elevated  
293 LcrF expression at 37°C, indicating that both proteins are needed to repress the *yscW-lcrF* promoter at  
294 mammalian body temperature. Although YmoA and the YmoA homolog Hha have been shown to bind DNA *in*  
295 *vitro*, YmoA and Hha lack a DNA binding domain and most likely purification of YmoA or Hha leads to  
296 copurification of H-NS or H-NS paralogs. This may explain why YmoA has been shown to interact with specific  
297 segments of DNA *in vitro*. Taken together, these data suggest that YmoA binding to H-NS does not alter H-NS  
298 occupancy at the *lcrF* promoter but, rather, potentiates H-NS repressive activity. *E. coli* Hha influences H-NS  
299 bridging and promotes H-NS silencing of target genes (36). We hypothesize that H-NS bound to YmoA forms a  
300 bridging complex on the *lcrF* promoter that represses *lcrF* transcription, and IscR disrupts this repressive  
301 complex. Testing this hypothesis will be the subject of future work.

302  
303 The mechanism by which IscR promotes or represses transcription of target genes varies. For example,  
304 elevated transcription of *ydiU*, a gene of unknown function, in *E. coli* is thought to be driven by direct  
305 interaction between RNA polymerase and IscR (41). However, IscR has also been shown to activate  
306 transcription of other target genes by antagonizing a repressor (45). For example, in *Vibrio vulnificus* IscR  
307 promotes expression of the *vvhBA* operon, which encodes an extracellular pore-forming toxin essential for its

308 hemolytic activity (45,64,65), while the *vvhBA* operon is repressed by H-NS (66). In *V. vulnificus*, nitrosative  
309 stress and iron starvation lead to upregulation of IscR (45). This increase in IscR leads to upregulation of  
310 *vvhBA* by increasing IscR levels and antagonizing H-NS repression of *vvhBA*. This molecular mechanism is  
311 very similar to what we observe here for IscR and H-NS in *Yersinia*, where aerobic conditions promote high  
312 IscR levels that antagonize H-NS repressive activity at the *yscW-IcrF* promoter. Therefore, antagonizing H-NS  
313 repression may be a common mechanism of gene regulation by IscR in response to changes in iron and  
314 oxygen.

315

## 316 **Materials and Methods**

### 317 **Bacterial strains and growth conditions**

318 Bacterial strains used in this paper are listed in Table S1. *Y. pseudotuberculosis* were grown, unless otherwise  
319 specified, in LB (Luria Broth) at 26°C shaking overnight. To induce the T3SS, overnight cultures were diluted  
320 into low calcium LB medium (LB plus 20 mM sodium oxalate and 20 mM MgCl<sub>2</sub>) to an optical density (OD<sub>600</sub>)  
321 of 0.2 and grown for 1.5 h at 26°C shaking followed by 1.5 h at 37°C to induce Yop synthesis, depending on  
322 the assay, as previously described (1).

323

324 For growing *Yersinia* under varying oxygen conditions, casamino acid-supplemented M9 media, referred to as  
325 M9 below, was used (2). Growth of cultures to vary oxygen tension was achieved by first diluting 26°C  
326 overnight aerobic cultures of *Y. pseudotuberculosis* to an OD<sub>600</sub> of 0.1 in fresh M9 minimal media  
327 supplemented with 0.9% glucose to maximize growth rate and energy production under anaerobic conditions,  
328 and incubating for 12 hrs under either aerobic or anaerobic conditions at 26°C. Both aerobic and anaerobic  
329 cultures were diluted to an OD<sub>600</sub> of 0.1, grown for 2 hrs at 26°C, and then shifted to 37°C for 4 hrs.

330

### 331 **Construction of *Yersinia* mutant strains**

332 The *Yersinia* mutants were generated as described in (3). H-NS was tagged with a C-terminal 3xFLAG affinity  
333 tag at the native locus through splicing by overlap extension (4), using primer pair *Fhns\_cds/Rhns\_cds* (Table  
334 S2) to amplify ~500bp upstream of *hns* plus the *hns* coding region excluding the stop codon,

335 F3xFLAG/R3xFLAG to amplify the 3xFLAG tag, and F3'*hns*/R3'*hns* to amplify the ~500 bp downstream region  
336 of *hns* including the stop codon. For the  $\Delta ymoA$  mutant, primer pairs F5/R5 $\Delta ymoA$  were used to amplify ~1000  
337 bp 5' of *ymoA* and F3/R3 $\Delta ymoA$  to amplify ~1000 bp 3' of *ymoA*. To generate the *ymoA*<sup>D43N</sup> mutant, primer  
338 pairs pUC19\_YmoA\_F and pUC19\_YmoA\_R were used to amplify 250 bp upstream of *ymoA* to 250  
339 downstream of the *ymoA* start codon and the amplified product cloned into a BamHI and SacI digested pUC19  
340 plasmid. Q5 site directed mutagenesis was performed using primer pairs *ymoA*<sup>D43N</sup>\_F and *ymoA*<sup>D43N</sup>\_R. The  
341 resulting plasmid, pUC19 *ymoA*<sup>D43N</sup>, was digested with BamHI and SacI and the resulting fragment was ligated  
342 into the suicide plasmid pSR47s. Mutant strains were generated as described above.

343  
344 In order to generate *lacZ* promoter constructs of *ymoBA* and *hns*, primer pairs  
345 pFU99a\_ymoA\_F/pFU99a\_ymoA\_R and pFU99a\_hns\_F/pFU99a\_hns\_R were used to amplify ~500 bp  
346 upstream of *ymoA* and *hns*, respectively, which included the first ten amino acids of *ymoA* and *hns*. These  
347 promoters and first ten amino acids of YmoA and H-NS were fused in frame to *lacZ* and cloned into a BamHI-  
348 and Sall-digested pFU99a using the NEBuilder HiFi DNA Assembly kit (New England Biolabs, Inc)  
349 electroporated into *Y. pseudotuberculosis*.

350  
351 In order to generate *lacZ* promoter constructs of *yscW-lcrF*, the reverse primer pFU99a\_yscWlcrF\_R was used  
352 with the following forward primers: pFU99a\_yscWlcrF\_p1 (promoter construct 1/-505 to +294 of *yscW*),  
353 pFU99a\_yscWlcrF\_p2 (promoter construct 2/ -309 to +294 of *yscW*), pFU99a\_yscWlcrF\_p3 (promoter  
354 construct 3/ -166 to +294 of *yscW*), pFU99a\_yscWlcrF\_p4 (promoter construct 4/ -47 to +294 of *yscW*), or  
355 pFU99a\_yscWlcrF\_p5 (promoter construct 5/ +101 to +294 of *yscW*). These promoter fragments were cloned  
356 into a BamHI- and Sall-digested pFU99a and electroporated into *Y. pseudotuberculosis*.

357

## 358 ***In vitro* transcription assay**

359 The DNA template used to assess if IscR could directly promote transcription of the *yscW-lcrF* promoter  
360 contained the -147 to +53 bp relative to the +1 transcription start site of *yscW*. The promoter containing the *Y.*  
361 *pseudotuberculosis* *sufA* promoter and the *E. coli* *sufA* promoter, which IscR has been shown to directly promote  
362 transcription of, served as a positive control (3, 5). The effect of IscR-C92A on  $\sigma$ 70-dependent activity was  
363 determined by incubating IscR-C92A with 2 nM supercoiled pPK12778 [purified with the QIAfilter Maxi kit

364 (Qiagen)], 0.25  $\mu$ Ci of [ $\alpha$ -<sup>32</sup>P]UTP (3,000  $\mu$ Ci/mmol; Perkin Elmer), 20  $\mu$ M UTP, and 500  $\mu$ M each of ATP, GTP,  
365 and CTP for 30 min at 37°C in 40 mM Tris (pH 7.9), 30 mM KCl, 10 mM MgCl<sub>2</sub>, 100  $\mu$ g/mL bovine serum albumin  
366 (BSA), and 1 mM DTT. Purified apo-IscR was used since the IscR binding site upstream of *yscW-lcrF* has been  
367 characterized to be an IscR type II site, which apo-IscR is capable of binding (6, 7). E $\sigma$ 70 RNA polymerase  
368 (NEB) was added to a final concentration of 50 nM and the reaction was terminated after 5 min by addition of  
369 Stop Solution (USB Scientific). Samples were heated for 60 s at 90°C, and loaded onto a 7 M urea-8%  
370 polyacrylamide gel in 0.5 $\times$  Tris-borate-EDTA (TBE) buffer. The reaction products were visualized by  
371 phosphorimaging.

372

### 373 **Type III secretion system secretion assay**

374 Visualization of T3SS cargo secreted in broth culture was performed as previously described (8). Briefly, *Y.*  
375 *pseudotuberculosis* in LB low calcium media (LB plus 20 mM sodium oxalate and 20 mM MgCl<sub>2</sub>) was grown for  
376 1.5 h at 26°C followed by growth at 37°C for 1.5 h. Cultures were normalized to OD<sub>600</sub> and pelleted at 13,200  
377 rpm for 10 min at room temperature. Supernatants were removed and proteins precipitated by addition of  
378 trichloroacetic acid (TCA) at a final concentration of 10%. Samples were incubated on ice for at least 1 hr and  
379 pelleted at 13,200 rpm for 15 min at 4°C. Resulting pellets were washed twice with ice-cold 100% acetone and  
380 resuspended in final sample buffer (FSB) containing 0.2 M dithiothreitol (DTT). Samples were boiled for 5 min  
381 prior to separating on a 12.5% SDS-PAGE gel. Coomassie stained gels were imaged using Bio-Rad Image Lab  
382 Software Quantity and Analysis tools. YopE bands were quantified using this software and normalized to the  
383 BSA protein precipitation control.

384

### 385 **Western Blot Analysis**

386 Cell pellets were collected, resuspended in FSB plus 0.2 M DTT, and boiled for fifteen minutes. At the time of  
387 loading, supernatants and cell pellets were normalized to the same number of cells. After separation on a 12.5%  
388 SDS-PAGE gel, proteins were transferred onto a blotting membrane (Immobilon-P) with a wet mini trans-blot  
389 cell (Bio-Rad). Blots were blocked for an hour in Tris-buffered saline with Tween 20 and 5% skim milk, and  
390 probed with the rabbit anti-RpoA (gift from Melanie Marketon), rabbit anti-LcrF (gift from Gregory Plano), rabbit  
391 anti-IscR (9), rabbit anti-YmoA (gift from Gregory Plano), rabbit anti-H-NS (gift from Robert Landick), mouse M2

392 anti-FLAG (Sigma), goat anti-YopE (Santa Cruz Biotech), and horseradish peroxidase-conjugated secondary  
393 antibodies (Santa Cruz Biotech). Following visualization, quantification of the bands was performed with Image  
394 Lab software (Bio-Rad).

395

## 396 **Quantitative RT-PCR**

397 RT-qPCR was carried out as previously described (3) using the primers in Table S2. The expression levels of  
398 each target gene were normalized to that of 16S rRNA present in each sample and calculated by utilization of a  
399 standard curve. At least three independent biological replicates were analyzed for each condition.

400

## 401 **$\beta$ -galactosidase Assays**

402 *Y. pseudotuberculosis* harboring promoter-*lacZ* fusion plasmids were grown in LB low calcium media (LB plus  
403 20 mM sodium oxalate and 20 mM MgCl<sub>2</sub>) for 1.5 h at 26°C followed by growth at 37°C for 1.5 h. Protein  
404 expression was stopped by incubating cells on ice for 20 minutes. Cultures were spun down and resuspended  
405 in Z Buffer (10). Samples were permeabilized using chloroform and 0.1% sodium dodecyl sulfate, incubated  
406 with 0.8 mg/mL ONPG, and  $\beta$ -galactosidase enzymatic activity was terminated by the addition of 1M sodium  
407 bicarbonate.  $\beta$ -galactosidase activity is reported as Miller units.

408

## 409 **CRISPRi knockdown**

410 Knockdown of H-NS via CRISPRi methods was adapted from (11). In order to generate the pgRNA-tetO-JTetR-  
411 H-NS plasmid, a protospacer-adjacent motif (PAM) was located near the promoter of *hns* (12). Two  
412 oligonucleotides (*hns\_gRNA\_F* and *hns\_gRNA\_R*) consisting of 20-nt targeting the *hns* promoter region with  
413 BbsI cohesive ends were synthesized and annealed before being cloned into pgRNA-tetO-JTetR by Golden  
414 Gate assembly. The plasmids pdCas9-bacteria and pgRNA-tetO-JTetR-H-NS were transformed into WT *Y.*  
415 *pseudotuberculosis* sequentially. These plasmids induce expression of dCas9 and gRNA-H-NS when exposed  
416 to anhydrotetracycline. *Y. pseudotuberculosis* cultures carrying these plasmids were sub-cultured to OD<sub>600</sub> 0.2  
417 and incubated at 26°C for 3 hrs in the presence or absence of 1 $\mu$ g/mL anhydrotetracycline, and then transferred  
418 to 37°C for 1.5 hrs to induce the T3SS. Samples were collected, and RNA was isolated for qRT-PCR analysis.

419

420

421

## 422 **Bioinformatic prediction of YmoA/H-NS binding sites**

423 A training set of known H-NS binding sites in *E. coli* K-12 substr. MG1655 from RegulonDB was used to generate  
424 an H-NS binding motif using MEME-suite 5.1.1 tools (13, 14). FIMO was then used to scan for an H-NS binding  
425 site near the regulatory region of the *yscW-lcrF* promoter.

426

## 427 **ChIP-qPCR**

428 Cells were grown for 3hrs at 26°C or 37°C with shaking at 250 rpm and protein/nucleic acids were crosslinked  
429 using 1% formaldehyde at 26°C or 37°C for 10 min. Crosslinking was quenched with the addition of ice cold 0.1  
430 M glycine and incubated at 4°C for 30 min. 32x1OD<sub>600</sub> cells were harvested for each replicate and cell pellets  
431 were stored at -80°C. DNA was fragmented by resuspending samples using IP buffer (100mM Tris-HCl, pH 8,  
432 300mM NaCl, 1% Triton X-100, 1 mM PMSF) and sonicated at 25% Amplitude 15s on/ 59s off for a total of 8  
433 cycles per sample. After sonication, lysates were treated with micrococcal nuclease and RNase-A for 1hr at 4°C.  
434 Lysates were clarified via centrifugation at 13,000 rpm for 15 min at 4°C. Lysates were pre-cleared using  
435 Dynabeads Protein A/G for 3hr at 4°C. Immunoprecipitation was performed by adding Sigma monoclonal mouse  
436 anti-FLAG M2 antibody to samples and incubated overnight at 4°C. Dynabeads Protein A/G were added to  
437 samples and washes were performed to remove non-specific binding. After H-NS-DNA or IscR-DNA complexes  
438 were eluted, samples were placed at 65°C for 5 hr to reverse crosslinks. DNA was then purified using Qiagen  
439 PCR purification kit and input samples were diluted 1:100 while samples treated with antibody or control samples  
440 not treated with the antibody were diluted 1:5 and qPCR was performed to assess IscR/H-NS binding to  
441 promoters of interest. Percent input was calculated by the following equation:  $100 * 2^{CT_{input} - CT_{+AB}}$ .

442

## 443 **Funding**

444 This study was supported by National Institutes of Health (www.NIH.gov) grant R01AI119082 (to VA and PJK).  
445 DAB and PA received support from the National Human Genome Research Institute of the National Institutes



446 of Health under Award Number 4R25HG006836. The funders had no role in study design, data collection and  
447 analysis, decision to publish, or preparation of the manuscript.

448

## 449 **Data Availability**

450 All study data are included in the article and SI Appendix. All experimental data will be made available upon  
451 request.

452

## 453 **Acknowledgments**

454 We thank Gregory V. Plano (University of Miami Health System) for the YmoA antibody and Robert Landick  
455 (University of Wisconsin, Madison) for the H-NS antibody.

456

## 457 **References**

- 458 1. Deng W, Marshall NC, Rowland JL, McCoy JM, Worrall LJ, Santos AS, et al. Assembly, structure,  
459 function and regulation of type III secretion systems. *Nature Reviews Microbiology*. 2017.
- 460 2. Cornelis GR. The type III secretion injectisome. *Nature Reviews Microbiology*. 2006.
- 461 3. Viboud GI, Bliska JB. *Yersinia* outer proteins: Role in modulation of host cell signaling responses and  
462 pathogenesis. *Annual Review of Microbiology*. 2005.
- 463 4. Navarro L, Alto NM, Dixon JE. Functions of the *Yersinia* effector proteins in inhibiting host immune  
464 responses. *Current Opinion in Microbiology*. 2005.
- 465 5. Schubert KA, Xu Y, Shao F, Auerbuch V. The *Yersinia* Type III Secretion System as a Tool for  
466 Studying Cytosolic Innate Immune Surveillance. *Annual Review of Microbiology*. 2020.
- 467 6. Pha K. *Yersinia* type III effectors perturb host innate immune responses . *World J Biol Chem*. 2016;
- 468 7. Brubaker RR. The Vwa+ virulence factor of yersiniae: the molecular basis of the attendant nutritional  
469 requirement for Ca<sup>++</sup>. *Reviews of infectious diseases*. 1983.
- 470 8. Milne-Davies B, Helbig C, Wimmi S, Cheng DWC, Paczia N, Diepold A. Life After Secretion—*Yersinia*  
471 *enterocolitica* Rapidly Toggles Effector Secretion and Can Resume Cell Division in Response to  
472 Changing External Conditions. *Front Microbiol*. 2019;

- 473 9. Brodsky IE, Medzhitov R. Reduced secretion of YopJ by *Yersinia* limits in vivo cell death but enhances  
474 bacterial virulence. PLoS Pathog. 2008;
- 475 10. Cornelis GR, Boland A, Boyd AP, Geuijen C, Iriarte M, Neyt C, et al. The Virulence Plasmid of *Yersinia*,  
476 an Antihost Genome. Microbiol Mol Biol Rev. 1998;
- 477 11. Schwiesow L, Lam H, Dersch P, Auerbuch V. *Yersinia* type III secretion system master regulator LcrF.  
478 Journal of Bacteriology. 2016.
- 479 12. Hoe NP, Minion FC, Goguen JD. Temperature sensing in *Yersinia pestis*: Regulation of yopE  
480 transcription by lcrF. J Bacteriol. 1992;
- 481 13. Yother J, Chamness TW, Goguen JD. Temperature-controlled plasmid regulon associated with low  
482 calcium response in *Yersinia pestis*. J Bacteriol. 1986;
- 483 14. Liu L, Huang S, Fei K, Zhou W, Chen S, Hu Y. Characterization of the binding motif for the T3SS  
484 master regulator LcrF in *Yersinia pseudotuberculosis*. FEMS Microbiol Lett. 2021;
- 485 15. King JM, Bartra SS, Plano G, Yahr TL. ExsA and LcrF recognize similar consensus binding sites, but  
486 differences in their oligomeric state influence interactions with promoter DNA. J Bacteriol. 2013;
- 487 16. Böhme K, Steinmann R, Kortmann J, Seekircher S, Heroven AK, Berger E, et al. Concerted actions of  
488 a thermo-labile regulator and a unique intergenic RNA thermosensor control *Yersinia* virulence. PLoS  
489 Pathog. 2012;
- 490 17. Hooker-Romero D, Mettert E, Schwiesow L, Balderas D, Alvarez PA, Kicin A, et al. Iron availability and  
491 oxygen tension regulate the *Yersinia* Ysc type III secretion system to enable disseminated infection.  
492 PLoS Pathog. 2019;
- 493 18. Shindo H, Ohnuki A, Ginba H, Katoh E, Ueguchi C, Mizuno T, et al. Identification of the DNA binding  
494 surface of H-NS protein from *Escherichia coli* by heteronuclear NMR spectroscopy. FEBS Lett. 1999;
- 495 19. Gordon BRG, Li Y, Cote A, Weirauch MT, Ding P, Hughes TR, et al. Structural basis for recognition of  
496 AT-rich DNA by unrelated xenogeneic silencing proteins. Proc Natl Acad Sci U S A. 2011;
- 497 20. Navarre WW, Porwollik S, Wang Y, McClelland M, Rosen H, Libby SJ, et al. Selective silencing of  
498 foreign DNA with low GC content by the H-NS protein in *Salmonella*. Science (80- ). 2006;
- 499 21. Dame RT, Luijsterburg MS, Krin E, Bertin PN, Wagner R, Wuite GJL. DNA bridging: A property shared  
500 among H-NS-like proteins. J Bacteriol. 2005;
- 501 22. Dame RT, Wyman C, Goosen N. H-NS mediated compaction of DNA visualised by atomic force

- 502 microscopy. *Nucleic Acids Res.* 2000;
- 503 23. Liu Y, Chen H, Kenney LJ, Yan J. A divalent switch drives H-NS/DNA-binding conformations between  
504 stiffening and bridging modes. *Genes Dev.* 2010;
- 505 24. Ono S, Goldberg MD, Olsson T, Esposito D, Hinton JCD, Ladbury JE. H-NS is a part of a thermally  
506 controlled mechanism for bacterial gene regulation. *Biochem J.* 2005;
- 507 25. Yang J, Tauschek M, Strugnell R, Robins-Browne RM. The H-NS protein represses transcription of the  
508 eltAB operon, which encodes heat-labile enterotoxin in enterotoxigenic *Escherichia coli*, by binding to  
509 regions downstream of the promoter. *Microbiology.* 2005;
- 510 26. Picker MA, Wing HJ. H-NS, its family members and their regulation of virulence genes in *Shigella*  
511 species. *Genes.* 2016.
- 512 27. Heroven AK, Nagel G, Tran HJ, Parr S, Dersch P. RovA is autoregulated and antagonizes H-NS-  
513 mediated silencing of invasin and rovA expression in *Yersinia pseudotuberculosis*. *Mol Microbiol.* 2004;
- 514 28. Ellison DW, Miller VL. H-NS represses inv transcription in *Yersinia enterocolitica* through competition  
515 with RovA and interaction with YmoA. *J Bacteriol.* 2006;
- 516 29. Cornelis GR. Role of the Transcription Activator VirF and the Histone-like Protein YmoA in the  
517 Thermoregulation of Virulence Functions in Yersiniae. *Zentralblatt fur Bakteriologie.* 1993;
- 518 30. Jackson MW, Silva-Herzog E, Plano G V. The ATP-dependent ClpXP and Lon proteases regulate  
519 expression of the *Yersinia pestis* type III secretion system via regulated proteolysis of YmoA, a small  
520 histone-like protein. *Mol Microbiol.* 2004;
- 521 31. Madrid C, Balsalobre C, García J, Juárez A. The novel Hha/YmoA family of nucleoid-associated  
522 proteins: Use of structural mimicry to modulate the activity of the H-NS family of proteins. *Molecular*  
523 *Microbiology.* 2007.
- 524 32. Nieto JM, Madrid C, Miquelay E, Parra JL, Rodríguez S, Juárez A. Evidence for direct protein-protein  
525 interaction between members of the enterobacterial Hha/YmoA and H-NS families of proteins. *J*  
526 *Bacteriol.* 2002;
- 527 33. Ali SS, Whitney JC, Stevenson J, Robinson H, Howell PL, Navarre WW. Structural insights into the  
528 regulation of foreign genes in salmonella by the Hha/H-NS complex. *J Biol Chem.* 2013;
- 529 34. Paytubi S, Madrid C, Fornis N, Nieto JM, Balsalobre C, Uhlin BE, et al. YdgT, the Hha paralogue in  
530 *Escherichia coli*, forms heteromeric complexes with H-NS and StpA. *Mol Microbiol.* 2004;

- 531 35. García J, Madrid C, Juárez A, Pons M. New Roles for Key Residues in Helices H1 and H2 of the  
532 *Escherichia coli* H-NS N-terminal Domain: H-NS Dimer Stabilization and Hha Binding. *J Mol Biol.* 2006;
- 533 36. Boudreau BA, Hron DR, Qin L, Van Der Valk RA, Kotlajich M V., Dame RT, et al. StpA and Hha  
534 stimulate pausing by RNA polymerase by promoting DNA-DNA bridging of H-NS filaments. *Nucleic*  
535 *Acids Res.* 2018;
- 536 37. Miller HK, Kwuan L, Schwiesow L, Bernick DL, Mettert E, Ramirez HA, et al. IscR Is Essential for  
537 *Yersinia pseudotuberculosis* Type III Secretion and Virulence. *PLoS Pathog.* 2014;
- 538 38. Rodionov DA, Gelfand MS, Todd JD, Curson ARJ, Johnston AWB. Computational reconstruction of  
539 iron- and manganese-responsive transcriptional networks in  $\alpha$ -proteobacteria. *PLoS Comput Biol.*  
540 2006;
- 541 39. Shepard W, Soutourina O, Courtois E, England P, Haouz A, Martin-Verstraete I. Insights into the Rrf2  
542 repressor family - The structure of CymR, the global cysteine regulator of *Bacillus subtilis*. *FEBS J.*  
543 2011;
- 544 40. Schwartz CJ, Giel JL, Patschkowski T, Luther C, Ruzicka FJ, Beinert H, et al. IscR, an Fe-S cluster-  
545 containing transcription factor, represses expression of *Escherichia coli* genes encoding Fe-S cluster  
546 assembly proteins. *Proc Natl Acad Sci U S A.* 2001;
- 547 41. Giel JL, Rodionov D, Liu M, Blattner FR, Kiley PJ. IscR-dependent gene expression links iron-sulphur  
548 cluster assembly to the control of O<sub>2</sub>-regulated genes in *Escherichia coli*. *Mol Microbiol.* 2006;
- 549 42. Nesbit AD, Giel JL, Rose JC, Kiley PJ. Sequence-Specific Binding to a Subset of IscR-Regulated  
550 Promoters Does Not Require IscR Fe-S Cluster Ligation. *J Mol Biol.* 2009;
- 551 43. Fleischhacker AS, Stubna A, Hsueh KL, Guo Y, Teter SJ, Rose JC, et al. Characterization of the [2Fe-  
552 2S] cluster of *Escherichia coli* transcription factor IscR. *Biochemistry.* 2012;
- 553 44. Schwartz CJ, Giel JL, Patschkowski T, Luther C, Ruzicka FJ, Beinert H, et al. IscR, an Fe-S cluster-  
554 containing transcription factor, represses expression of *Escherichia coli* genes encoding Fe-S cluster  
555 assembly proteins. *Proc Natl Acad Sci.* 2001;
- 556 45. Choi G, Jang KK, Lim JG, Lee ZW, Im H, Choi SH. The transcriptional regulator IscR integrates host-  
557 derived nitrosative stress and iron starvation in activation of the *vvhBA* operon in *Vibrio vulnificus*. *J*  
558 *Biol Chem.* 2020;
- 559 46. Cornells GR, Sluifers C, Delor I, Geib D, Kaniga K, de Rouvroit CL, et al. *ymoA*, a *Yersinia*

- 560 *enterocolitica* chromosomal gene modulating the expression of virulence functions. Mol Microbiol.  
561 1991;
- 562 47. de Rouvroit CL, Sluiter C, Cornelis GR. Role of the transcriptional activator, VirF, and temperature in  
563 the expression of the pYV plasmid genes of *Yersinia enterocolitica*. Mol Microbiol. 1992;
- 564 48. Cordeiro TN, García J, Bernadó P, Millet O, Pons M. A three-protein charge zipper stabilizes a  
565 complex modulating bacterial gene silencing. J Biol Chem. 2015;
- 566 49. Wang T, Wang M, Zhang Q, Cao S, Li X, Qi Z, et al. Reversible gene expression control in *Yersinia*  
567 *pestis* by using an optimized CRISPR interference system. Appl Environ Microbiol. 2019;
- 568 50. Chaparian RR, Tran MLN, Miller Conrad LC, Rusch DB, Van Kessel JC. Global H-NS counter-silencing  
569 by LuxR activates quorum sensing gene expression. Nucleic Acids Res. 2020;
- 570 51. Ayala JC, Wang H, Silva AJ, Benitez JA. Repression by H-NS of genes required for the biosynthesis of  
571 the *Vibrio cholerae* biofilm matrix is modulated by the second messenger cyclic diguanylic acid. Mol  
572 Microbiol. 2015;
- 573 52. Prosseda G, Fradiani PA, Di Lorenzo M, Falconi M, Micheli G, Casalino M, et al. A role for H-NS in the  
574 regulation of the virF gene of Shigella and enteroinvasive *Escherichia coli*. Res Microbiol. 1998;
- 575 53. Balderas D, Mettert E, Lam HN, Banerjee R, Gverzdys T, Alvarez P, et al. Genome Scale Analysis  
576 Reveals IscR Directly and Indirectly Regulates Virulence Factor Genes in Pathogenic *Yersinia*. MBio.  
577 2021;12(3):e00633-21.
- 578 54. Balada-Llasat JM, Meccas J. *Yersinia* has a tropism for B and T cell zones of lymph nodes that is  
579 independent of the type III secretion system. PLoS Pathog. 2006;
- 580 55. He G, Shankar RA, Chzhan M, Samouilov A, Kuppusamy P, Zweier JL. Noninvasive measurement of  
581 anatomic structure and intraluminal oxygenation in the gastrointestinal tract of living mice with spatial  
582 and spectral EPR imaging. Proc Natl Acad Sci U S A. 1999;
- 583 56. Rivera-Chávez F, Lopez CA, Bäumlér AJ. Oxygen as a driver of gut dysbiosis. Free Radical Biology  
584 and Medicine. 2017.
- 585 57. Cassat JE, Skaar EP. Iron in infection and immunity. Cell Host and Microbe. 2013.
- 586 58. Plano G V., Schesser K. The *Yersinia pestis* type III secretion system: Expression, assembly and role  
587 in the evasion of host defenses. Immunol Res. 2013;
- 588 59. Cornelis GR. Molecular and cell biology aspects of plague. Proc Natl Acad Sci U S A. 2000;

- 589 60. Schroeder GN, Hilbi H. Molecular pathogenesis of *Shigella* spp.: Controlling host cell signaling,  
590 invasion, and death by type III secretion. *Clinical Microbiology Reviews*. 2008.
- 591 61. Di Martino ML, Falconi M, Micheli G, Colonna B, Prosseda G. The multifaceted activity of the VirF  
592 regulatory protein in the *Shigella* Lifestyle. *Frontiers in Molecular Biosciences*. 2016.
- 593 62. Beloin C, McKenna S, Dorman CJ. Molecular dissection of VirB, a key regulator of the virulence  
594 cascade of *Shigella flexneri*. *J Biol Chem*. 2002;
- 595 63. Falconi M, Colonna B, Prosseda G, Micheli G, Gualerzi CO. Thermoregulation of *Shigella* and  
596 *Escherichia coli* EIEC pathogenicity. A temperature-dependent structural transition of DNA modulates  
597 accessibility of virF promoter to transcriptional repressor H-NS. *EMBO J*. 1998;
- 598 64. Gray LD, Kreger AS. Purification and characterization of an extracellular cytolysin produced by *Vibrio*  
599 *vulnificus*. *Infect Immun*. 1985;
- 600 65. Jeong HG, Satchell KJF. Additive function of vibrio vulnificus MARTXVv and VvhA cytolysins promotes  
601 rapid growth and epithelial tissue necrosis during intestinal infection. *PLoS Pathog*. 2012;
- 602 66. Elgaml A, Miyoshi SI. Role of the histone-like nucleoid structuring protein H-NS in the regulation of  
603 virulence factor expression and stress response in vibrio vulnificus. *Biocontrol Sci*. 2015;
- 604
- 605

## 606 **Supporting Information**

607 **Figure S1. YmoA affects LcrF dependent type III secretion activity.**

608 **Figure S2. YmoA mutations do not affect mRNA levels or protein levels of IscR or H-NS.**

609 **Figure S3. IscR does not regulate YmoA or H-NS expression.**

610 **Figure S4. 3xFLAG tag allows for detection of H-NS using FLAG antibody and does not affect H-NS**  
611 **ability to repress LcrF**

612 **Figure S5. IscR enrichment at the *suf* promoter is not influenced by temperature.**

613 **Table S1. Strains used in this study.**

614 **Table S2. *Y. pseudotuberculosis* primers used in this study.**

615 **Table S3. Plasmids used in this study.**

616

617

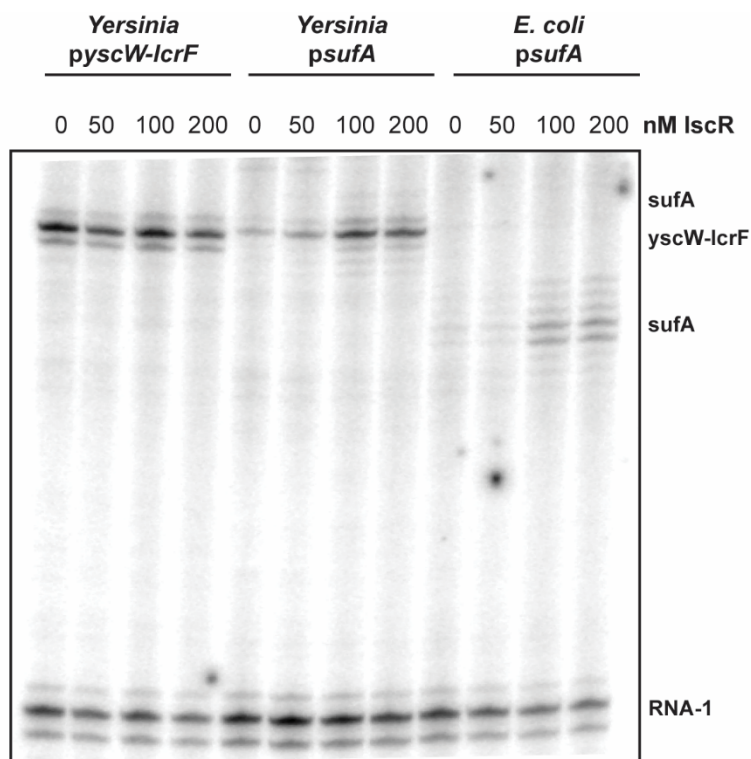
618

619

620

621

622



623

624 **Figure 1. IscR does not directly promote transcription of *yscW-IcrF* in vitro.** *In vitro* transcription

625 reactions containing plasmids encoding the promoter of interest (*yscW-IcrF*, *sufA*, or *E. coli* K12 MG1655

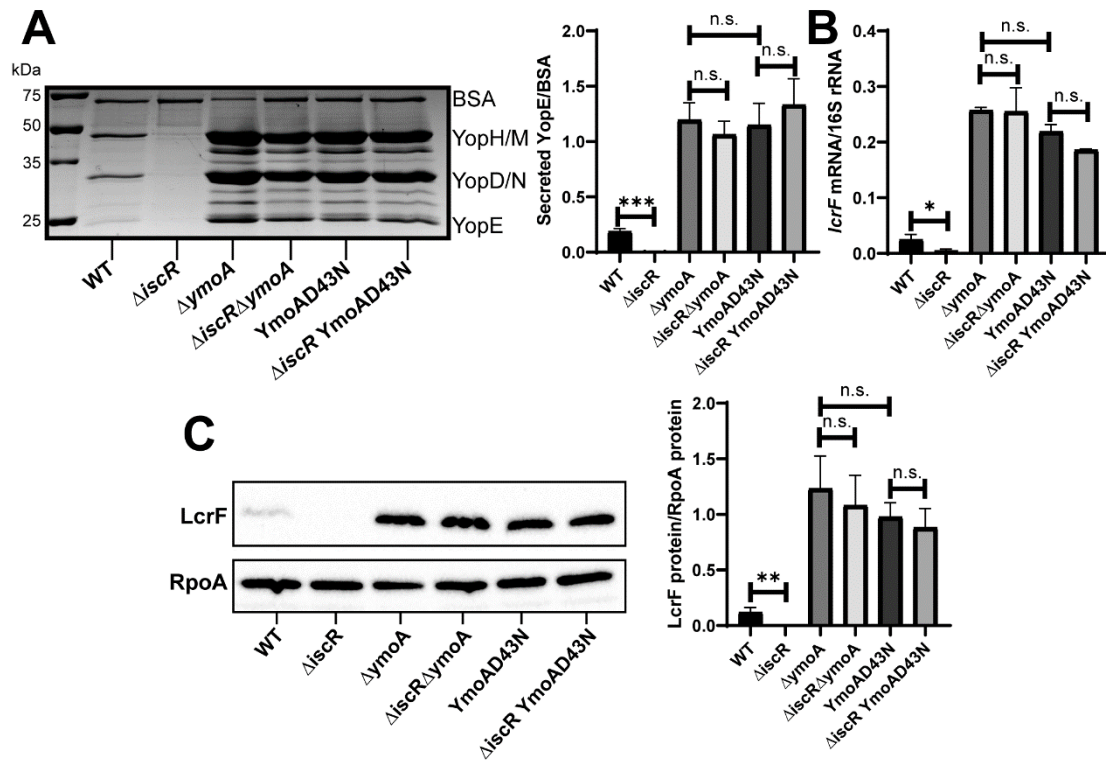
626 *sufA*), E $\sigma$ 70 RNA polymerase, and, where indicated, 50-200 nM IscR C92A protein lacking iron sulfur cluster

627 coordination were incubated and analyzed. RNA-1 served as a control for this experiment.

628

629

630



631

632 **Figure 2. IscR is dispensable for type III secretion in the  $\Delta$ ymoA mutant background.** *Yersinia* strains

633 were grown under T3SS-inducing conditions (low calcium at 37°C). (A) Precipitated secreted proteins were

634 visualized by SDS-PAGE followed by Coomassie blue staining. Bovine serum albumin (BSA) was used as a

635 loading control (left panel). Densitometry was used to measure the relative amount of secreted YopE T3SS

636 effector protein versus BSA control. The average of four independent replicates  $\pm$  standard deviation is shown

637 (right panel). (B) RNA was extracted and reverse transcriptase quantitative PCR (RT-qPCR) was used to

638 measure relative levels of *lcrF* mRNA normalized to 16S rRNA. The average of at least three biological

639 replicates are shown  $\pm$  standard deviation. (C) LcrF protein levels were determined by Western blotting (left

640 panel) and densitometry (right panel) relative to the RpoA loading control. Shown is the average of four

641 independent replicates  $\pm$  standard deviation. Statistical analysis was performed using an unpaired Student's t-

642 test (\* $p < .05$ , \*\* $p < .01$ , \*\*\* $p < .001$ , and n.s. non-significant).

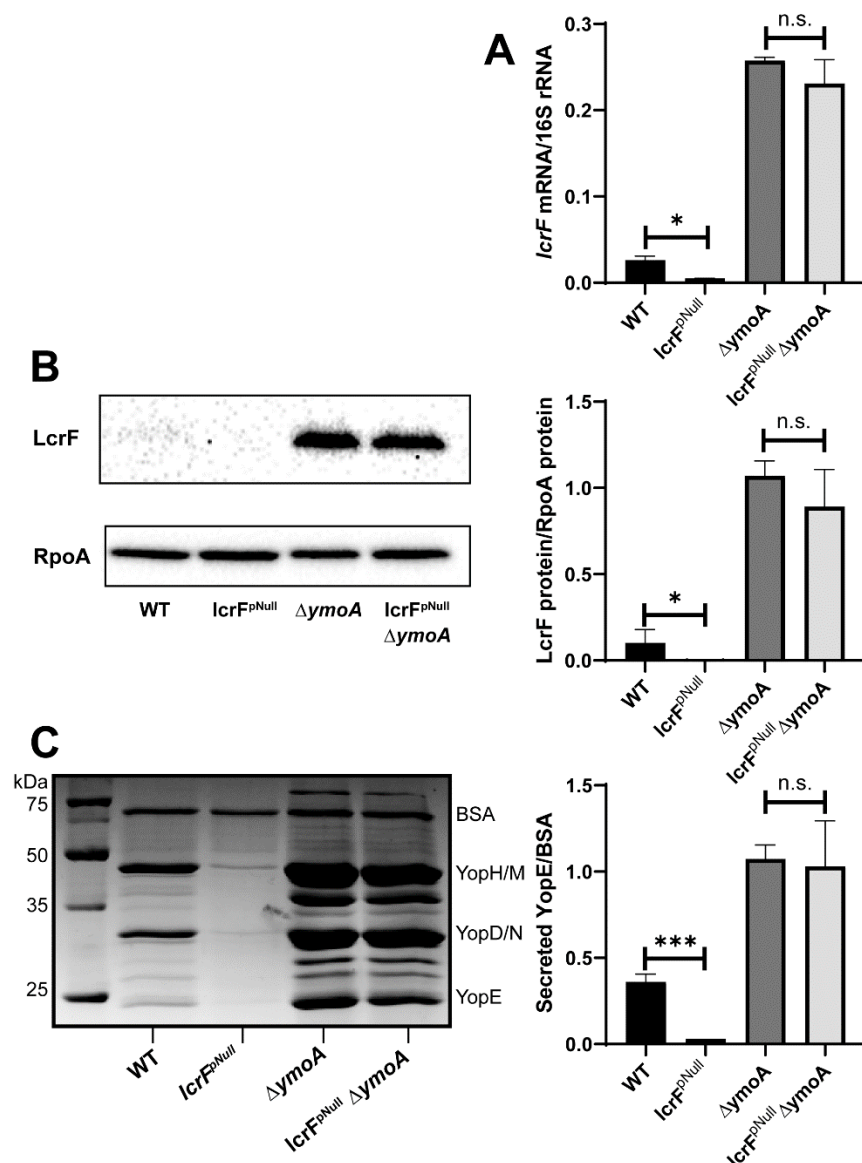
643

644

645

646





647

648 **Figure 3. IscR binding to the *yscW-IcrF* promoter is dispensable in the absence of *ymoA*. *Yersinia***

649 strains were grown under T3SS-inducing conditions. **(A)** Levels of *IcrF* mRNA were measured and normalized

650 to 16S rRNA using RT-qPCR. The average of at least three biological replicates are shown  $\pm$  standard

651 deviation. **(B)** LcrF protein levels were measured relative to the RpoA loading control by Western blotting (left

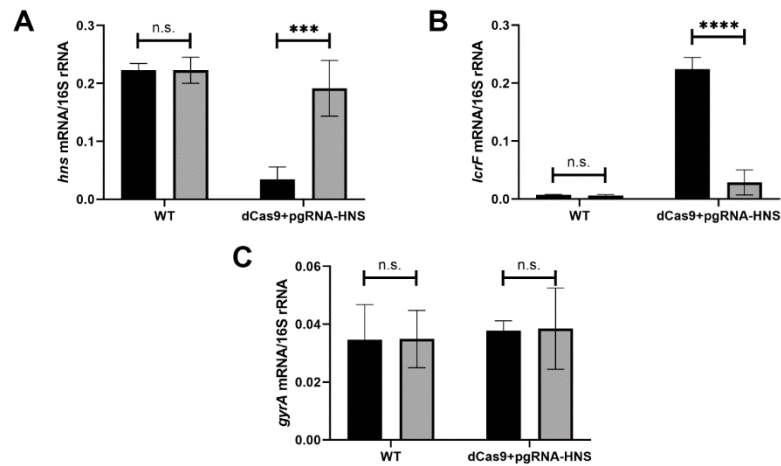
652 panel) and densitometry (right panel). Shown is the average of four biological replicates  $\pm$  standard deviation.

653 **(C)** Secreted proteins were precipitated and visualized by SDS-PAGE followed by Coomassie blue staining

654 (left panel). The YopE bands were normalized to the BSA loading control (right panel). The average of three

655 biological replicates  $\pm$  standard deviations are shown. Statistical analysis was performed using an unpaired

656 Student's t-test (\* $p < .05$ , \*\*\* $p < .001$ , and n.s. non-significant).



657

658 **Figure 4. Knockdown of H-NS leads to derepression of LcrF.** *Y. pseudotuberculosis* strains were grown in  
659 low calcium LB in the absence (grey bars) or presence (black bars) of 1 µg/mL anhydrotetracycline for 3 hrs at  
660 26°C to induce expression of *hns* guide RNA and dCas9 and then transferred to 37°C (T3SS inducing  
661 conditions) for 1.5 hrs. RNA was analyzed by RT-qPCR for *hns* (A), *lcrF* (B), or *gyrA* (C) mRNA level  
662 normalized to 16S rRNA. The average of three biological replicates are shown ± standard deviation. Statistical  
663 analysis was performed using an unpaired Student's t-test (\*\*\*p<.001, \*\*\*\*p<.0001, and n.s. non-significant).

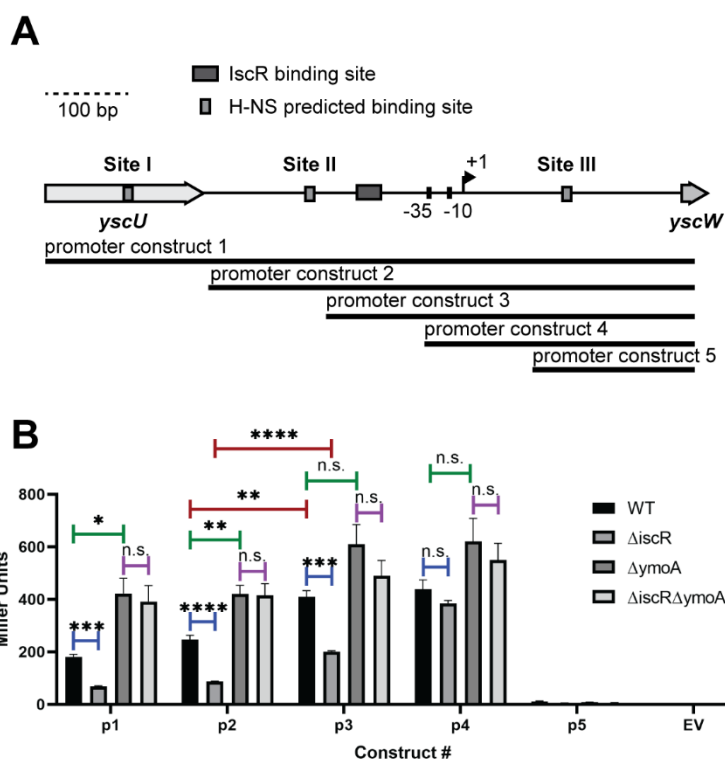
664

665

666

667

668



669

670 **Figure 5. Defining regulatory regions required for IscR and H-NS-YmoA control of PyscW-IcrF**

671 **expression. (A)** Diagram of the *yscW-IcrF* promoter region (800 bp) containing the known IscR binding site

672 (dark grey box), three MEME-suite FIMO predicted H-NS binding sites, referred to as Site I, Site II, and Site III

673 (light grey boxes) and the previously characterized transcriptional start site (arrow). Schematic of PyscW-

674 *IcrF::lacZ* fusions. Five constructs (p1-p5) were used to assess which regions of *pyscW-IcrF* allows for H-NS-

675 YmoA repression and IscR activation. **(B)** *Yersinia* harboring the various *pyscW-IcrF::lacZ* plasmids were

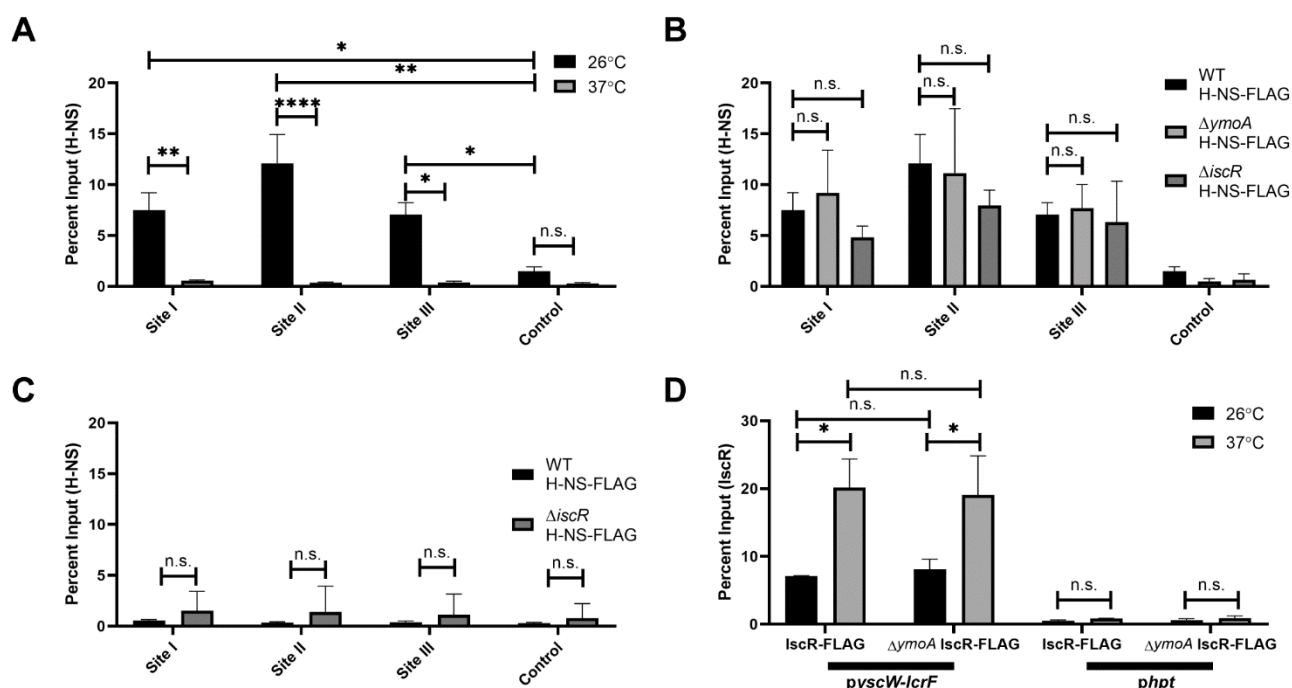
676 grown under T3SS-inducing conditions (low calcium LB at 37°C) for 1.5 hrs and assayed for β-galactosidase

677 (Miller units). The average of at least three biological replicates are shown ± standard deviation. Statistical

678 analysis was performed using an unpaired Student's t-test (\*p<.05, \*\*p<.01, \*\*\*p<.001, \*\*\*\*p<.0001, and n.s.

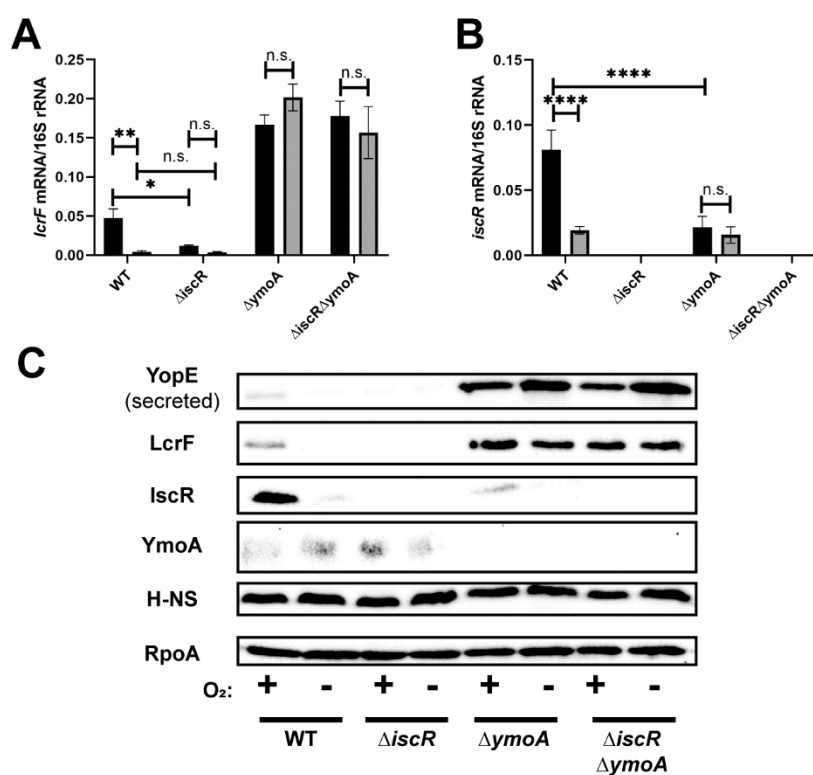
679 non-significant).

680



681

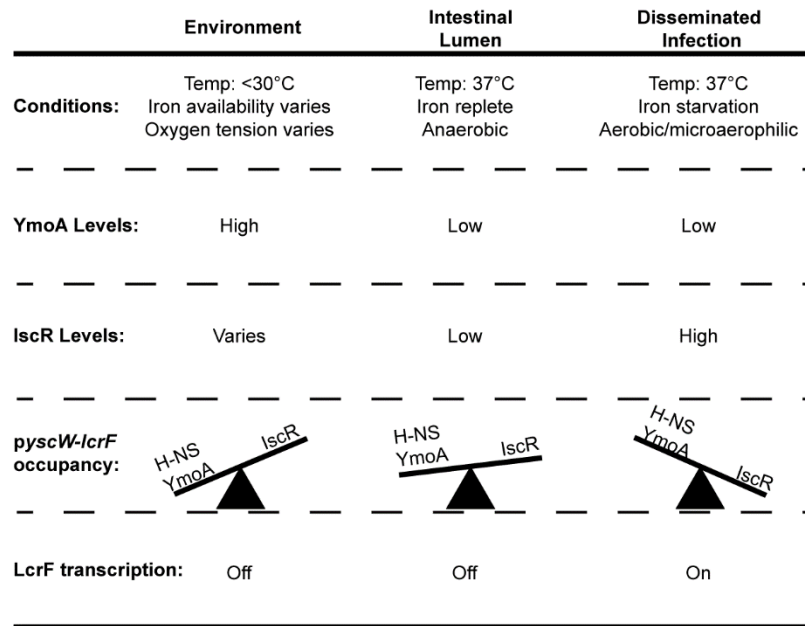
682 **Figure 6. H-NS and IscR bind to the *yscW-lcrF* promoter at different temperatures. (A)** The relative  
 683 enrichment (percent input) of Site I, Site II, and Site III promoter DNA and a control promoter (DN756\_21750),  
 684 which H-NS is not predicted to bind, was analyzed by anti-FLAG ChIP-qPCR in *Yersinia* expressing H-NS-  
 685 FLAG. ChIP-qPCR was performed with bacteria grown at 26°C (black bars) or 37°C (grey bars) in low calcium  
 686 LB for 3 hrs. The average of at least three biological replicates  $\pm$  standard deviation is shown. **(B)** ChIP-qPCR  
 687 was performed with the H-NS-FLAG allele in wildtype,  $\Delta ymoA$ , or  $\Delta iscR$  mutant background at 26°C **(C)** ChIP-  
 688 qPCR was performed with the H-NS-FLAG allele in wildtype or  $\Delta iscR$  mutant background at 37°C. The  
 689 average of at least three biological replicates  $\pm$  standard deviation is shown. **(D)** ChIP-qPCR was performed  
 690 with the *IscR-FLAG* allele in the wildtype or  $\Delta ymoA$  mutant background at 26°C (black bars) or 37°C (grey  
 691 bars). The *hpt* control promoter, which *IscR* is not predicted to bind, was used as a negative control. The  
 692 average of at least three biological replicates  $\pm$  standard deviation is shown and statistical analysis was  
 693 performed using Two-way ANOVA (\* $p < .05$ , \*\* $p < .01$ , \*\*\* $p < .001$ , \*\*\*\* $p < .0001$  and n.s. non-significant).



694

695 **Figure 7. Oxygen-dependent control of *IcrF* requires *YmoA*.** *Yersinia* strains were cultured under T3SS  
 696 inducing conditions under aerobic (black bars) or anaerobic (grey bars) conditions. Levels of *IcrF* (A) and  
 697 (B) mRNA levels were measured by RT-qPCR and normalized to 16S rRNA. The average of at three  
 698 biological replicates are shown  $\pm$  standard deviation. (C) *Yersinia* strains were grown under similar conditions  
 699 as stated above and whole cell extracts were probed for RpoA, IscR, H-NS, LcrF, YopE, and YmoA by  
 700 Western blotting. One representative experiment out of three biological replicates is shown. Statistical analysis  
 701 was performed using a one-way ANOVA with Tukey multiple comparisons (\* $p$ <.05, \*\* $p$ <.01, \*\*\*\* $p$ <.0001, and  
 702 n.s. non-significant).

703



704

705 **Figure 8. Proposed model for activation of *yscW-lcrF* via *IscR*** At environmental conditions (26°C, low  
 706 oxidative stress, high iron), H-NS occupancy at the *yscW-lcrF* promoter is high and LcrF expression and T3SS  
 707 activity is repressed. When *Y. pseudotuberculosis* becomes ingested, it travels to the intestinal lumen. YmoA  
 708 protein levels decrease due to ClpXP/Lon protease activity at 37°C, but sufficient levels remain to potentiate  
 709 H-NS-mediated repression of *yscW-lcrF* and prevent type III secretion. This is because *IscR* levels are kept  
 710 low by anaerobic and iron replete conditions. Once *Y. pseudotuberculosis* crosses the intestinal barrier, it  
 711 encounters higher oxygen tension and lower iron availability, causing an increase in *IscR* protein levels that  
 712 can antagonize YmoA/H-NS repression of *yscW-lcrF* and allow for LcrF expression and T3SS activity.

713

714

715

716